Tag Modulation Silencing: Design and Application in RFID Anti-Collision Protocols

Abdallah Alma'aitah, *Member, IEEE*, Hossam S. Hassanein, *Senior Member, IEEE*, and Mohamed Ibnkahla, *Member, IEEE*

***Abstract*—Reliable and energy-efficient reading of Radio Frequency IDentification (RFID) tags is of utmost importance, especially in mobile and dense tag settings. We identify tag collisions as a main source of inefficiency in terms of wasting both medium access control (MAC) frame slots and reader's energy. We propose modulation silencing (MS), a reader-tag interaction framework to limit the effect of tag collisions. Utilizing relatively simple circuitry at the tag, MS enhances the performance of existing anti-collision protocols by allowing readers to terminate collision slots once a decoding violation is detected. With shorter collision slots, we revisit the performance metrics and introduce a new generalized time efficiency metric and an optimal frame selection formula that takes into consideration the MS effects. Through analytical solutions and extensive simulations, we show that the use of MS results in significant performance gains under various scenarios.**

***Index Terms*—RFID, anti-collision, Continous Wave (CW), passive tags, frame optimization, collision slots, tag identification.**

I. Introduction

RFID technology provides fast and non-line-of-sight data collection that enables several automatic inventory applications [1]. In these applications, RFID tags are attached to a large number of objects, and the unique identifiers (IDs) of these tags are collected by executing an anti-collision protocol at fixed or mobile readers. Improving the time and power efficiencies of anti-collision protocols is a key challenge which in turn extends the lifetime of battery powered readers.

The tags in RFID systems are low power integrated circuits with an antenna interface. The antenna facilitates both energy harvesting of the reader's Continuous Wave (CW) signal and communication with the reader on a half-duplex channel. On this channel, the tag either receives the reader's commands or sends its own data by selective backscattering the reader's CW. Due to the limited available power for passive RFID tags, tag-to-tag coordination and data relaying are challenging in typical passive tags. Therefore, the reader acts as a central powerful node that is responsible for collecting the tags' data, organizing their replies, and limiting simultaneous replies (collisions). Nevertheless, even using optimal settings of up-to-date anti-collision protocols, collisions contribute to 26%–50% of the total time slots [2]–[5].

In a given time slot, if more than one tag reply simultaneously, the reader is forced to wait until these tags conclude their reply. This is because the half-duplex channel between the tags and the reader prevents them from decoding any command during their data backscattering [6], [7]. In this paper, we propose a novel collision resolution approach, called Modulation Silencing (MS), in which the reader can significantly reduce the time of collision slots.

In MS, once the reader detects a collision it terminates its CW transmission. The tags, in turn, are equipped with a CW detection circuitry that stops the ongoing selective backscattering if the CW is absent. MS targets the reduction of collision slots and is applicable for any time-slotted probabilistic (ALOHA-based) or deterministic (Tree-based) protocol. Analytical solutions and simulation results show that MS significantly enhances reading time. A higher throughput enables higher speeds of reading both mobile and transient tags. In addition, faster reading indicates shorter activation of the reader's RF components (e.g., amplifiers, mixers, and modulators), which is a crucial factor in the lifetime of mobile battery powered readers.

Our contributions in this article are as follows: For RFID readers, we propose Rapid Collision Detection (RCD) that allows CW termination when a collision is detected. At the tag, Continuous Wave Absence Detection (CWAD) is proposed. We present a generalized time system efficiency metric that considers the shorter collision slots. We obtain a closed form expression to calculate the optimal identification frame size in ALOHA-based protocols. We evaluate, by analytical solutions and simulations, the effect of MS on the efficiency of time-slotted anti-collision protocols.

The remainder of this paper is organized as follows. In Section II, we introduce the collision problem and related work. In Section III we introduce modulation silencing components and their effect on collision slot duration. Analytical and simulation performance analyses are given in Section IV. In Section V the paper is concluded and future outlook of modulation silencing is given.

II. Motivation and Related Work

A. Motivation

In passive RFID systems, time-slotted anti-collision protocols are the state-of-the art identification protocols and the main

Manuscript received January 8, 2014; revised June 10, 2014 and August 27, 2014; accepted August 31, 2014. Date of publication October 9, 2014; date of current version November 18, 2014. This work was supported by a grant from the Natural Sciences and Engineering Research Council (NSERC) of Canada. The associate editor coordinating the review of this paper and approving it for publication was P. Popovski.

A. Alma'aitah and H. S. Hassanein are with the School of Computing, Queen's University, Kingston, ON K7L 2N8, Canada (e-mail: 8aa14@queensu.ca; hossam@cs.queensu.ca).

M. Ibnkahla is with the Department of Electrical and Computer Engineering, Queen's University, Kingston, ON K7L 3N6, Canada (e-mail: ibnkahla@queensu.ca).

Color versions of one or more of the figures in this paper are available online at http://ieeexplore.ieee.org.

Digital Object Identifier 10.1109/TCOMM.2014.2356581

stream schemes that are extensively researched. Optimally, the reader's command should address a single tag. However at times either no tags or multiples of tags may respond to the same command. In case of a single tag reply (single slot), the reader decodes the reply and acknowledges (ACK) the tag if the reply is error free; otherwise, negative acknowledgment (NACK) is sent. If no tags reply (empty slot), the reader in some protocols [8] might "early end" the slot to save time and power. In case that multiple tags reply simultaneously (collision slot), the reader sends a NACK after the tags conclude their selective backscattering. Such a slot is wasted, and overcoming this scenario is the main focus of this work.

Unlike empty slots, a reader is unable to terminate or "early end" collision slots since:

- Sending a stop command to the tags will not be decoded, since passive RFID systems use half-duplex (HDX) communication channel [6], [7].
- Stopping its CW transmission to save power will reset tags, because all tags (even the tags which are not replying in that specific slot) are harvesting power from CW. Stopping the CW until the replying tags finish their backscattering will cause tags to reset their states (due to voltage drop).
- Ignoring the current slot and initiating a new slot may cause another collision, since the tags in the current collision slot are still modulating their data. Starting a new slot will cause another collision with replies in the newly initiated slot.

Our motivation lies in the significant detriment of collision slots in tag identification and the potential time and power saving if collision time is reduced.

B. Related Work

The time efficiency enhancements in previous anti-collision protocols are mainly focused on reducing the *number* of collided slots in the overall slots. In ALOHA-based protocols, this reduction is achieved by estimating the tag count to select the optimal frame size [9]–[11]. In ISO/IEC 18000-3 Mode 1 Extended Mode Standard [12], the cyclic redundancy check (CRC) of the tag's message is processed if there are no encoding violations as EPC Class1 Gen 2 standards [13]. However, if a decoding violation (collision) is detected in the message it skips CRC and issues a NACK. Nevertheless, the reader waits, it skips CRC processing without time reduction of the collision slot, for the tags to conclude their transmissions to issue the NACK.

In EPC Class 1 Gen 2 standard [13], a two-phase tag identification mechanism is adopted to reduce the effect of empty and collision slots. In the first phase, the tag backscatters a relatively short random sequence (compared to the tag's ID) to the reader. If this sequence is error free, the reader initiates the second phase by sending the same sequence back to the tag. Then the tag sends its full ID. If the first phase contains multiple replies or no reply, the second phase will not be executed. This scheme reduces the time of both empty and collision slots; however, the time of the first phase is added to every single reply. As verified by Dobkin [6], the length of the first phase is comparable to the second phase; hence, the longer single time slots hinders the gain of shorter collision and empty slots [6].

Recently, Kang *et al.* [14] and Khasgiwale *et al.* [15] proposed collision direct decoding schemes for the EPC standard. These schemes modify the random sequence reply of the tag to allow information extraction. In case of a collision, the received signal at the reader is expected to be corrupt at specific bits of the random sequence allowing the reader to determine one of the sequences correctly. However, the modification to the tag reply requires software and hardware changes at both reader and tags. In addition, the possible combinations of the random sequence in [15] are limited for easier information extraction, which limits the maximum number of tags that can be supported by this scheme.

Tree-based protocols provide a comparable performance to the most efficient ALOHA-based protocols. In Tree-based protocols [5], [16], [17], stacks and tables are employed at both readers and tags to prevent visiting tree nodes, which causes repeated collisions. Lui *et al.* [4] propose Smart Trend Traversal (STT) protocol that outperformed other Tree-based protocols by following the tags' ID clusters in the binary tree to minimize empty and collision slots. STT achieves superior performance by moving horizontally in the tree (at the same depth) after every single reply slot. However, such performance is achieved at nearly full trees which is not the case in practice. For instance, as a 96-bit ID space constructs a binary tree of 2^{96} leaves, the reported results in [4] requires having 2^{90} to 2^{96} tags within the vicinity of the reader, which is not practical. Therefore, in typical tag populations, that ranges from a few tags to a few thousand tags (i.e., 2^{10}–2^{12}), the performance of STT converges to the expected performance of other binary Tree-based protocols [5], [16], [17].

Existing protocols either target the reduction of collisions in the overall slots or attempt to extract data from collision slots. The former has theoretical limits that cannot be exceeded due to the nature of random replies of the tags that lack intercommunication. The latter requires additional complex hardware interface at the reader and *a priori* knowledge of parts of transmitted data. We propose a mechanism that imitates a full duplex communication channel between tags and readers to allow tag reply termination in collision slots. This mechanism mainly targets reducing the collision *time* and is, therefore, applicable to all time-slotted anti-collision protocols. To the best of our knowledge, no existing work has considered collision duration reduction or tag reply termination.

C. Time Slot Structure

To lay the groundwork for evaluating the effectiveness of MS in time-slotted protocols, the main time slot parameters in RFID protocols are described in this section.

In passive RFID systems, the reader starts the communication with the surrounding tags by sending a CW to power them up. The tags rectify the CW signal and store the voltage in a relatively large capacitor. The tags need a continuous power feed at the antenna to stay on and remain synchronized with the reader. Therefore, the reader's command symbols are sent as Pulse Interval Encoding (PIE) (a method to send data and

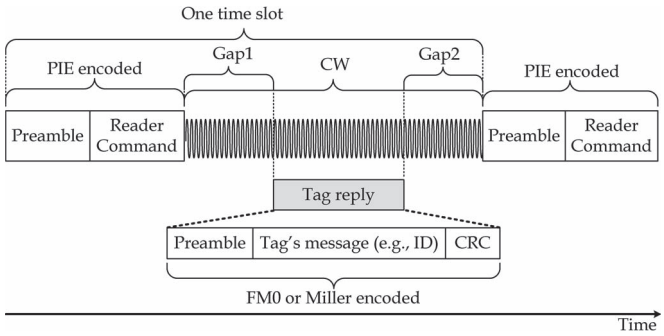

Fig. 1. Time slot data fields in reader-tag-reader communication.

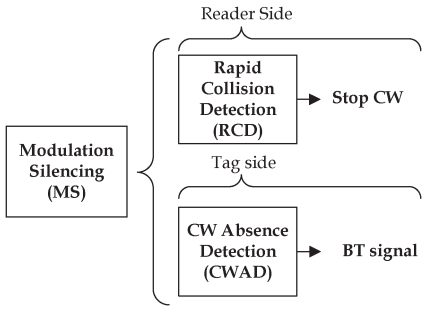

Fig. 2. Modulation Silencing (MS) components.

energy at the same time). PIE has variable energy intervals that can be harvested by the tag's rectifier while decoding the reader's data. After the command, the CW is turned on and the reader is ready to hear the modulated echo of the CW from the replying tag antenna. The replying tag encodes its data in FM0 (or Miller) encoding; the tag alternates its antenna impedance based on the "low" and "high" periods of the data. The impedance affects reflected power and/or phase of the CW from the tag's antenna which allows the reader to decode the tag's symbols.

The *data-fields* of the time slot structure are shown in Fig. 1. The reader initiates the slot by a command followed by a gap period. The length of this gap is designed to allow command processing at the tag and to accommodate transmission delays (due to tag IC variations and distance from the reader). The tag reply begins with a preamble followed by the tag's message. The message is typically appended with CRC for error detection. Another gap period follows the tag reply to allow CRC processing at the reader. The reader then sends a single command to positively acknowledge or negatively acknowledge the tag's message and possibly, to initiate a new slot.

The exact timing of the *data-fields* differs according to several protocol-specific parameters. In our performance evaluation we consider the timing parameters specified in the EPC Class 1 Gen 2 standard [13] for tag symbol length, reader symbol length, gaps ranges, and preamble lengths.

III. Modulation Silencing

The proposed mechanism allows readers to inform the tags of collisions by turning off CW transmission.[1] If a collision is detected, the reader stops CW transmission for a predefined period. Within this period, the tags detect the absence of CW and stop their ongoing data modulation. This tag-reader coordination allows the interpretation of a stop signal from the reader to the tag on a half-duplex channel. In MS, we model collision slot duration ($\mathrm{T_c^{MS}}$) as

$$\mathrm{T_c^{MS}} = \mathrm{T_{com}} + \mathrm{T_{gap}} + (\mathrm{H}+1)\mathrm{T_{sym}} + \mathrm{T_{CWAD}} + \mathrm{T_{sym}}, \quad (1)$$

where $\mathrm{T_{com}}$, $\mathrm{T_{gap}}$, and $\mathrm{T_{sym}}$ are command, gap, and tag-to-reader symbol durations, respectively. H is the expected number of correctly decoded bits before detecting an error (encoding violation). $\mathrm{T_{CWAD}}$ is the required time by the tag to detect reader's CW cutoff. The last term in (1) is one symbol duration for sensing the channel in case some tags were not silenced within $\mathrm{T_{CWAD}}$.

In the following, we introduce MS components and define H and $\mathrm{T_{CWAD}}$. MS components are illustrated in Fig. 2. The readers execute Rapid Collision Detection (RCD) after every command. The tags sense the reader's CW signal by the Continuous Wave Absence Detection (CWAD) circuit. CWAD circuitry interrupts the tag's ongoing data modulation by asserting the Backscattering Termination (BT) signal.

A. MS at the Reader

For RFID readers, Rapid Collision Detection (RCD) is applied to stop CW once a collision is detected. In collision slots, receiving different symbols from two or more tags violates the encoding scheme [14]. These violations indicate an erroneous message even before checking its CRC.

The RCD algorithm is presented in Algorithm 1. The reader sends a command to initiate the slot then starts emitting its CW to be backscattered by the addressed tag. A tag starts the reply by sending a preamble followed by its message. When M tags reply simultaneously, we denote the kth symbol from a tag $\mathrm{m} \in \mathrm{M}$ as $\mathrm{S_m^k}$. If the reader did not detect any error in the tag transmission, it continues CW transmission and receives the whole message including CRC. If the reader did not detect a reply, it ends the slot and starts a new one if needed. In the case of collision slots, the received signals from the tag to the reader are either bit-level unsynchronized or synchronized. An example of a collision with $\mathrm{M} = 3$ tags is given in Fig. 3 for unsynchronized and synchronized transmissions. Unsynchronized transmissions can be due to the difference in distances from the tags to the reader or due to a tag's chip variations factors (e.g., different clock oscillation).

Algorithm 1 Rapid Collision Detection (RCD) at the reader

1: **Send Command, Start CW**
2: **after** Gap_1
3: **if** *backscattering is detected* **then**
4: $\mathrm{j} = 0$;
5: **while** *backscattering is* True **do**
6: **if** $reply[j] = unexpected\ violation$ **then**
7: Stop CW for $\mathrm{T_{CWAD}}$

[1] A simplified version of MS appeared in [18].

```
8:        Start CW and sense the channel
9:        if backscattering is detected then
10:           go to 5
11:       else
12:           go to 1
13:       end if
14:     else
15:       j = j + 1
16:     end if
17:   end while
18:   if CRCmatch = true then
19:     Send L sequence with ACK
20:     Take protocol-specific action
21:     go to 1
22:   else
23:     Send NACK
24:   end if
25: else
26:   go to 1
27: end if
```

In the event of unsynchronized transmissions, decoding errors are experienced in all overlapped symbols [6], including preamble symbols.

In case of bit-level synchronization, the preamble bits {Pre} are decoded correctly since

$$\mathrm{S}_0^{\mathrm{k}} = \mathrm{S}_1^{\mathrm{k}} = \cdots = \mathrm{S}_{\mathrm{M}}^{\mathrm{k}} \; \forall \, \mathrm{k} \in \{\mathrm{Pre}\} \; [6].$$

Decoding errors are detected when at least one symbol value is different than the symbols from the $\mathrm{M}-1$ tags. Nevertheless, the M tags might send long bit sequences before they start sending different bits. Therefore, a random sequence of L bits is appended after the preamble to increase the probability of earlier detection of an encoding violation.

In a collision slot, once an error is detected in the L sequence, the reader stops CW transmission for $\mathrm{T_{CWAD}}$ that is sufficient to trigger the BT signal at the tag. Then the reader sends a command negatively acknowledging the previous transmission. If the reader receives an error free L sequence, it keeps its CW on until it detects an error in the message.

The length of the random sequence is crucial for collision detection. During a collision slot from M tags, the probability p of having at least one different bit from the $\mathrm{m^{th}}$ tag at the $\mathrm{k^{th}}$ symbol is

$$\begin{aligned} \mathrm{p} &= 1 - \Pr\left(\mathrm{S}_1^{\mathrm{k}} = \mathrm{S}_2^{\mathrm{k}} = \cdots = \mathrm{S}_{\mathrm{M}}^{\mathrm{k}}\right) \\ &= 1 - 2 \prod_{\mathrm{m}=1}^{\mathrm{m}=\mathrm{M}} \left(\frac{1}{2}\right) = 1 - \left(\frac{1}{2}\right)^{\mathrm{M}-1}. \end{aligned} \tag{2}$$

Consequently, the probability of having M tags sending the same kth symbol is $\mathrm{q} = 1 - \mathrm{p}$. Therefore, the expected number of correctly decoded bits H from M tags before the end of L is

$$\mathrm{H} = \sum_{\mathrm{k}=1}^{\mathrm{k}=\mathrm{L}} \mathrm{kpq^k} \approx 1/\mathrm{p} \text{ for large L.} \tag{3}$$

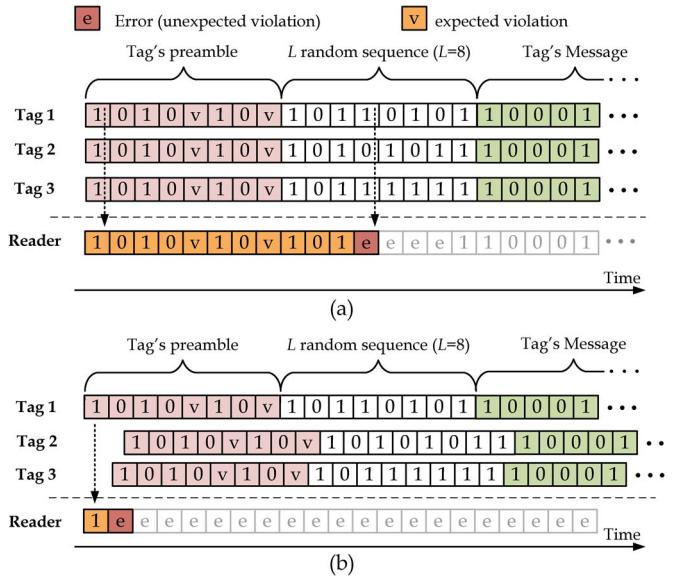

Fig. 3. Error detection for three tags sending their preamble and random sequence to the reader. (a) Syncronized replies. (b) Unsynchronized replies.

In the example in Fig. 3, each tag transmits a preamble (as in of EPC Class 1 Gen 2 standard [13]) followed by its $L = 8$ random sequence and its message. In the standard [13], the preamble intentionally contains violations to distinguish the preamble from the tag's data. In RCD algorithm, these violations are skipped and will not trigger an error to turn the CW off. If the reply from multiple tags are bit-level synchronized (which is highly unlikely in RFID systems [6]) as in the example of Fig. 3(a), the first error is detected after the preamble (at the fourth bit of the L sequence in Fig. 3(a)). In unsynchronized replies (as in the example in Fig. 3(b)), the error is detected much earlier because an unexpected violation will be experienced during the preamble (in the second bit of Fig. 3(b)). In both cases, once an error is detected the reader discontinues its CW transmission for a period of $\mathrm{T_{CWAD}}$.

1) Design Considerations: When tags reply from different distances, the reply with the strongest signal may overshadow other replies, be correctly decoded, and be acknowledged. In such case, the distant tags (with weaker signals) will assume that the acknowledgment is addressed to them, which reduces system reliability. In RCD, we adopt the EPC Class 1 Gen 2 method [13] in eliminating the near-far problem by sending the L sequence back in the acknowledgment to ensure that it is only targeted to the tag with matching sequence.

Normally, after $\mathrm{T_{CWAD}}$ all tags should stop their selective backscattering. However, due to integrated circuits (ICs) process variations, some tags may have faulty CWAD circuits that do not detect the CW cutoff within $\mathrm{T_{CWAD}}$. Therefore, RCD accommodates such tags by resuming CW transmission after $\mathrm{T_{CWAD}}$ and sensing the channel for any ongoing reply (lines 7–10 in Algorithm 1).

B. MS at the Tag

MS is achieved when the tag is able to detect the CW cutoff by the reader. A block diagram of the basic components in passive tags is shown in Fig. 4.

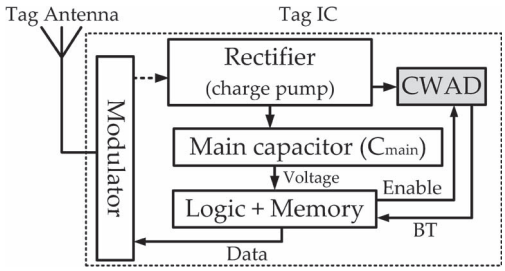

Fig. 4. Main components of passive RFID tag with CWAD circuit.

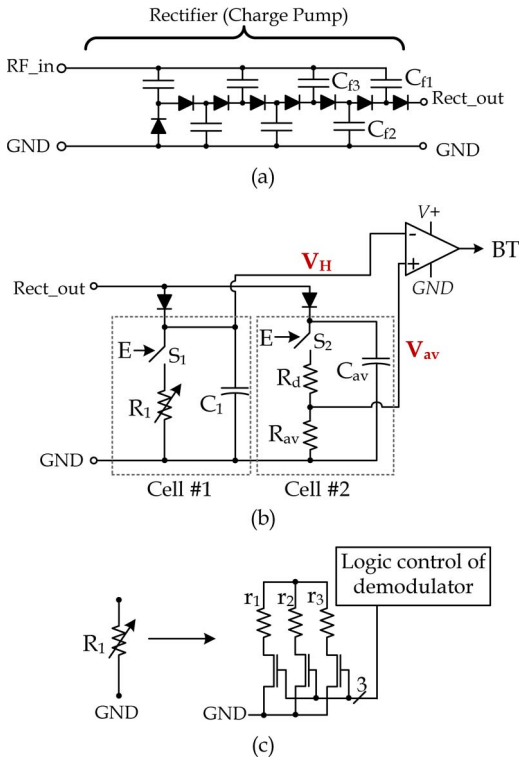

Fig. 5. (a) Tag's voltage rectifier (3 stages Dickson charge pump). (b) CWAD circuit schematic showing its basic components. (c) Components of the switched resistor R_1.

The tag's rectifier and the CWAD circuit are illustrated in Fig. 5(a) and (b), respectively. CWAD consists of two RC cells and is placed after the rectifier to sense the CW signal. The first RC cell in Fig. 5(b) provides an envelope detection of the output voltage from the rectifier, noted as V_H. The second RC cell provides the average voltage of the rectifier's output, noted as V_{av}. The envelope detector capacitor C_1 is smaller than the averaging capacitor C_{av}. The pull down resistor of the envelop detector cell (R_1) is also smaller than the combined resistors in the averaging cell $(R_d + R_{av})$. The pull-down resistors are activated by two active high switches S_1 and S_2. Note that the two RC cells in Fig. 5 are isolated by two diodes to allow independent discharging as will be discussed shortly. R_d and R_{av} are used to divide the voltage across C_{av}. The cells outputs, V_H and V_{av}, are compared by a voltage comparator that is triggered to assert the BT signal when V_H is lower than V_{av} by the comparator switching threshold V_{diff}.

1) CWAD Operation: When tags are powered up, the voltages across C_1 and C_{av} are equal to the rectifier's output voltage. An illustration of CWAD operation is given in Fig. 6.

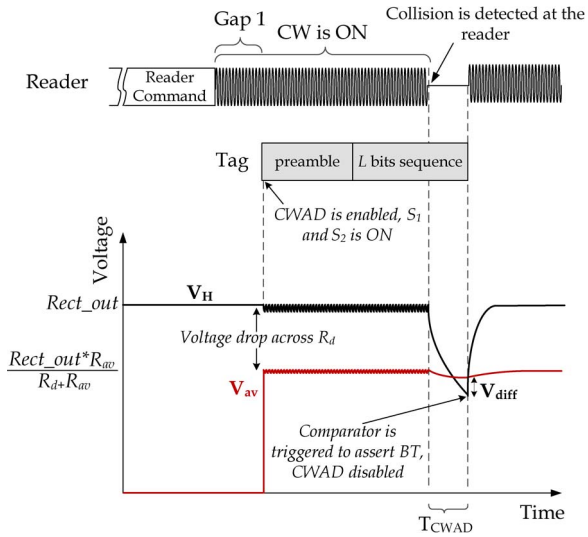

Fig. 6. Illustrative example of the voltage across R_1 (i.e., V_H) and R_{av} (i.e., V_{av}).

The reader starts the slot by sending a command followed by CW transmission. After receiving the reader's command, all tags enable their CWAD circuit by asserting the enable signal E to turn on the switches S_1 and S_2. The addressed tag(s) by the reader command start selective backscattering the preamble followed by their data. Since the voltage at C_{av} and C_1 are the same (i.e., equals to V_H), V_{av} is less than V_H by the drop accross R_d as shown in Fig. 6. Closing the switches S_1 and S_2 allows C_1 and C_{av} to discharge their voltage in R_1 and $(R_d + R_{av})$, respectively. At the same time, C_1 and C_{av} are being charged from the output of the rectifier as long as CW is still on.

If the reader detects a collision and stops its CW transmission, C_1 will discharge its voltage in R_1 at a higher rate than C_{av} in $(R_d + R_{av})$. Once V_H is less than $V_{av} - V_{diff}$, the comparator triggers a BT signal.

If an ACK or NACK is received, the tag deactivates the CWAD circuit and takes a protocol-specific action. The protocol action for ACK or NACK may differ. For instance, in ALOHA-based protocols a NACK puts the tag in a mute state until the next frame is issued. In Tree-based protocols, a NACK may change the state counters in all tags. To address the near-far issue, the tag checks if the L sequence in the ACK matches its sequence. The L sequence generation has no design overhead as existing tags are already designed with random number generation circuits [5].

2) CWAD Timing: To ensure a proper operation of CWAD, BT signal must be triggered within the CW cutoff period T_{CWAD}. Rapid detection of the CW cutoff is desirable, however, since tags with amplitude modulation selective backscattering do not rectify any power during transmission of HIGH periods of backscattered symbols [19], T_{CWAD} must be longer than these HIGH periods to prevent triggering BT in every HIGH period of symbols transmission.[2]

[2]Tags that use Phase Modulation (PM) for backscattering harvest power in LOW and HIGH periods of the backscattered symbols, hence no lower limit of T_{CWAD} is required.

Since the symbol duration from the tag to the reader (denoted as T_{pri} in the EPC standard) is set by the reader during communication initialization. The value of R_1 in CWAD is changed to accommodate the different tag symbol duration. We take advantage of the already available control lines in the control of the demodulator in the tag [19]. The control lines are used to switch the transistors in Fig. 5(c) to provide different resistance values from the parallel resistors r_1, r_2, and r_3. Similar to the demodulator switched resistor, R_1 is switched to larger values in longer T_{pri} durations and vice versa.

In our design, T_{CWAD} is selected to be, at least, twice the HIGH period in tag's symbols. In the EPC standard, the HIGH period $(T_{pri}/2)$ can be as low as 0.78 μs and as high as 12.5 μs [13].

3) Rectifier Capacitance Effect: As CWAD is connected to the output of the rectifier, it is important to ensure that the rectifiers capacitance is not affecting the time required to trigger BT. When CW is cutoff, V_H starts falling with a time constant $\tau = R_1C_1$; however, this is not the only time constant that controls the drop of V_H. V_H drops from $2u(V_{in} - V_{th})$, where u is the number of stages in the charge pump rectifier, V_{in} is the input peak voltage at the tag antenna, and V_{th} is the threshold voltage of the diodes in the rectifier. A drop of $(V_{in} - V_{in})$ in V_H turns on the diode touching C_1 because of the higher voltage at the capacitor C_{f1} from the last stage of the rectifier of Fig. 5. In such case, C_{f1} in parallel with C_1 will be discharging over R_1. Another drop of $(V_{in} - V_{th})$ in V_H allows C_{f2} to start discharging in R_1, and so on. Fig. 7 presents a simulation of CWAD operation and the effect of the rectifier's capacitors on T_{CWAD}.

The voltage V_H is dropping at a variable rates due to the increased capacitance at every drop of $(V_{in} - V_{in})$. The voltage drop for the first three time constants is expressed in (4), shown at the bottom of the page. The time constants in (4) are $\tau_1 = R_1C_1$, $\tau_2 = R_1(C_1 + C_{f1})$, and $\tau_3 = R_1(C_1 + C_{f1} + C_{f2})$. The three points in (4) are depicted in the waveform in Fig. 7. On the other hand, the drop of V_{av} is affected by the large time constant $\tau_{V_{av}} = (R_d + R_{av})R_{av}$, which is stable compared to the drop in V_H.

By considering all the parameters that can affect the duration of T_{CWAD}, a precise set of T_{CWAD} values can be accommodated for each value of T_{pri} (Table I). By referring to Fig. 7, to eliminate the effect of the rectifier capacitance, V_{av} can be designed to be very close to V_H by making $R_d \ll R_{av}$. This reduction in R_d allows V_H to drop below V_{av} while being affected by τ_1.

It is worth mentioning that CWAD circuit design overhead is negligible when compared to the complexity of passive RFID tags. CWAD circuit contains two capacitors (area consuming elements) and few transistors and resistors. The two capacitors

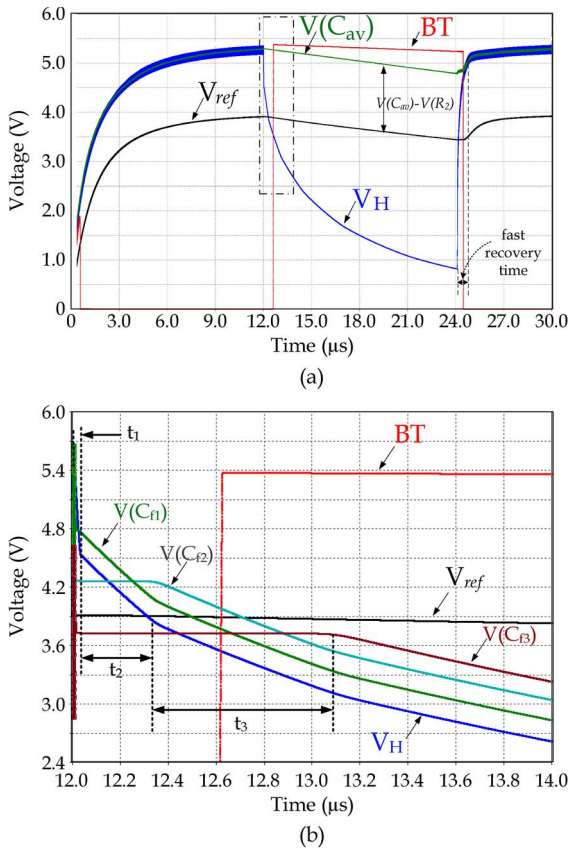

Fig. 7. Simulation of CWAD and the effect of the rectifiers capacitors on the detection time T_{CWAD}.

TABLE I
CWAD COMPONENTS VALUES THAT ENSURE $T_{pri} < T_{CWAD} < 2T_{pri}$

Component	smallest $T_{pri}/2$ (0.78μs)	largest $T_{pri}/2$ (12.5μs)
R_1	1MΩ	17MΩ
R_{av}	45MΩ	45MΩ
R_d	5MΩ	5MΩ
C_1	15pf	15pf
R_{av}	70pf	70pf
V_{diff}	50mV	50mV

are two orders of magnitude less than the main capacitor and the rectifier capacitance [20]. On the other hand, transistors and resistors of CWAD pose an insignificant addition to the transistor numbers the logic and memory of passive RFID tags [20], [21].

Based on RCD and CWAD circuit, T_c^{MS} in (1) can be precisely evaluated. In this section we have defined the two parameters that affect collision slots length in MS: the expected number of bits before the first error (H), and CW cutoff detection time T_{CWAD}. In the following section we analyze the

$$V_H = \begin{cases} V_{max}e^{t/\tau_1}, & \text{if } 0 < t < -\tau_1 \ln\left(\frac{V_{max}-V_{in}+V_{th}}{V_{max}}\right) = t_1 \\ (V_{max} - V_{in} + V_{th})e^{t/\tau_2}, & \text{if } t_1 < t < -\tau_2 \ln\left(\frac{V_{max}-2V_{in}+2V_{th}}{V_{max}-V_{in}+V_{th}}\right) = t_2 \\ (V_{max} - 2V_{in} + 2V_{th})e^{t/\tau_3}, & \text{if } t_2 < t < -\tau_3 \ln\left(\frac{V_{max}-3V_{in}+3V_{th}}{V_{max}-2V_{in}+2V_{th}}\right) = t_3 \end{cases} \quad (4)$$

effect of these shorter collision slots on the overall throughput and time efficiency of anti-collision protocols.

IV. MS Performance Evaluation

In this section, we evaluate the effect of shorter collision slots enabled by MS on time slotted protocols. First, we define a new time efficiency metric that consider shorter collision slots. Second, we provide analytical solutions that captures performance improvement of MS in anti-collision protocols. Last, we simulate ALOHA- and Tree- based protocols with and without MS under standardized time slot parameters.

A. Performance Metrics

Current time efficiency metrics do not consider the time difference between single and collision slots (i.e., $\mathrm{T_c} = \mathrm{T_s}$). To evaluate the time efficiency of protocols that utilize MS, performance metrics that take into account the time difference between the slots are required. Recently, a Time System Efficiency (TSE) metric was proposed by La Porta *et al.* [2] with consideration to shorter empty slots. TSE is given as

$$\begin{aligned}\mathrm{TSE} &= \frac{\mathrm{R_s T_s}}{\mathrm{R_e T_e} + \mathrm{R_s T_s} + \mathrm{R_c T_c}},\\ &= \frac{\mathrm{R_s}}{\beta \mathrm{R_e} + \mathrm{R_s} + \mathrm{R_c}},\end{aligned}$$

where β is the ratio of empty slot duration (T_e) to single slot duration (T_s), R_s, R_e, and R_c are the total number of single, empty, and collision slots, respectively. As collision slots are shorter with MS, we generalize TSE metric to include collision to single slot duration ratio, denoted by γ, where

$$\gamma = \frac{\mathrm{T_c}}{\mathrm{T_s}} < 1.$$

The generalized TSE $(\mathrm{TSE_g})$ metric is expressed as

$$\mathrm{TSE_g} = \frac{\mathrm{R_s}}{\gamma \mathrm{R_c} + \mathrm{R_s} + \beta \mathrm{R_e}}.$$

Throughput, in terms of tags per unit of time, is another powerful indicator on the protocol's efficiency. Throughput (TH) is expressed as

$$\begin{aligned}\mathrm{TH} &= \frac{\mathrm{R_s}}{\mathrm{R_c T_c} + \mathrm{R_s T_s} + \mathrm{R_e T_e}}\\ &= \frac{\mathrm{R_s}}{\left(\mathrm{R_c}\frac{\mathrm{T_c}}{\mathrm{T_s}} + \mathrm{R_s} + \mathrm{R_e}\frac{\mathrm{T_e}}{\mathrm{T_s}}\right)\mathrm{T_s}}\\ &= \frac{\mathrm{TSE_g}}{\mathrm{T_s}},\end{aligned}$$

In the following we evaluate different protocols under three possible scenarios: i) "No Early Ending" of empty and collision slots, denoted as "NEE" $(\mathrm{T_e} = \mathrm{T_c} = \mathrm{T_s})$), ii) "Early Ending of Empty" slots is applied, denoted as "EEE" $(\mathrm{T_e} < \mathrm{T_c} = \mathrm{T_s})$, iii) When MS is applied to end empty and collision slots, denoted as "MS" $(\mathrm{T_e} < \mathrm{T_c} < \mathrm{T_s})$.

B. Analytical Solution

In this section we provide formalization for MS effect on time efficiency improvement in terms of the previously defined metrics. In addition, we provide an optimal frame selection closed-form that is specific to ALOHA-based protocols. This formalization provides the analytical base on which we compare the simulation results that will be obtained in Section IV-C.

1) MS Temporal Improvement: To analyze MS time efficiency improvement over non-MS protocols, γ is the main factor in defining such improvement. In addition, we consider the probability of undetected collision within the L sequence, $\mathrm{w} = \mathrm{p}^L$, in our analysis. Let $\mathrm{z} = 1 - \mathrm{w}$ be the probability of collision detection within the L sequence. Note that the probability of not detecting a collision slot is w (undetected collision slots will have a length of a single slot $\mathrm{T_s}$). Therefore, there will be $\mathrm{wR_c}$ undetected collision slots that have a total time of $\mathrm{wR_c T_s}$. In addition, we denote the ratios of total collision and empty slots to single slots as $\mathrm{a} = \mathrm{R_e}/\mathrm{R_s}$ and $\mathrm{b} = \mathrm{R_c}/\mathrm{R_s}$. Therefore, $\mathrm{TSE_g}$ for MS, NEE, and EEE can be written as

$$\mathrm{TSE_g^{MS}} = \frac{1}{(1+\mathrm{w}) + \beta\mathrm{a} + \mathrm{z}\gamma\mathrm{b}}, \tag{5}$$

$$\mathrm{TSE_g^{NEE}} = \frac{1}{1+\mathrm{a}+\mathrm{b}}, \tag{6}$$

and

$$\mathrm{TSE_g^{EEE}} = \frac{1}{1+\beta\mathrm{a}+\mathrm{b}}, \tag{7}$$

respectively.

From (5) and (6), $\mathrm{TSE_g}$ improvement of MS over NEE is

$$\frac{\mathrm{TSE_g^{MS}} - \mathrm{TSE_g^{NEE}}}{\mathrm{TSE_g^{NEE}}} = \frac{\mathrm{b}(1-\mathrm{z}\gamma) + \mathrm{a}(1-\beta) - \mathrm{w}}{1 + \mathrm{w} + z\gamma\mathrm{b} + \beta\mathrm{a}}. \tag{8}$$

Consequently, throughput improvement of MS over NEE $\mathrm{TH^{MS}} - \mathrm{TH^{NEE}}/\mathrm{TH^{NEE}})$ is

$$\frac{\mathrm{T_s^{NEE}} + \mathrm{b}\left(\mathrm{T_s^{NEE}} - \mathrm{T_s^{MS}}\mathrm{z}\gamma\right) + \mathrm{a}\left(\mathrm{T_s^{NEE}} - \mathrm{T_s^{MS}}\beta\right) - \mathrm{T_s^{MS}}(1-w)}{\mathrm{T_s^{MS}}(1 + \mathrm{w} + \mathrm{z}\gamma\mathrm{b} + \beta\mathrm{a})}. \tag{9}$$

Note that we have differentiated $\mathrm{T_c^{MS}}$ from $\mathrm{T_c^{NEE}}$ as their length may not be the same. Similarly, From (5) and (7), $\mathrm{TSE_g}$ improvement of MS over EEE is

$$\frac{\mathrm{TSE_g^{MS}} - \mathrm{TSE_g^{EEE}}}{\mathrm{TSE_g^{EEE}}} = \frac{\mathrm{b}(1-\mathrm{z}\gamma) - \mathrm{w}}{1 + \mathrm{w} + \mathrm{z}\gamma\mathrm{b} + \beta\mathrm{a}}, \tag{10}$$

and the throughput improvement of MS over EEE $(\frac{\mathrm{TH^{MS}} - \mathrm{TH^{EEE}}}{\mathrm{TH^{EEE}}})$ is

$$\frac{\mathrm{T_s^{EEE}} + \mathrm{b}\left(\mathrm{T_s^{EEE}} - \mathrm{T_s^{MS}}\mathrm{z}\gamma\right) + \mathrm{a}\beta\left(\mathrm{T_s^{EEE}} - \mathrm{T_s^{MS}}\right) - \mathrm{T_s^{MS}}(1-\mathrm{w})}{\mathrm{T_s^{MS}}(1 + \mathrm{w} + \mathrm{z}\gamma\mathrm{b} + \beta\mathrm{a})}. \tag{11}$$

TH improvement converges to $\mathrm{TSE_g}$ improvement when $\mathrm{T_s^{MS}} = \mathrm{T_s^{non-MS}}$. In the following we conduct extensive simulations to support our analytical solution above.

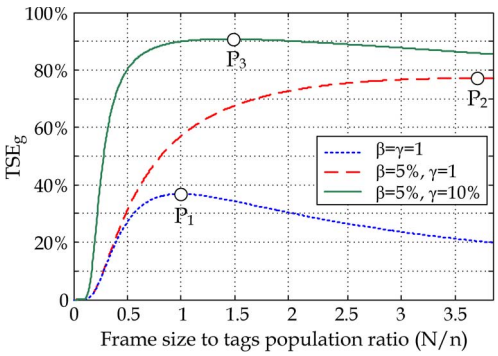

Fig. 8. γ and β effects on the peak's location and value of $\mathrm{TSE_g}$.

2) Optimal Frame Selection: Even though the previous analytical solutions are sufficient for capturing the effect on shorter collision slots on the performance of anti-collision protocols, further analysis for ALOHA-based protocols is needed as time efficiency of such protocols depends on selecting the optimal frame size $\mathrm{N_{optimal}}$ [22]. Since the optimal frame size is selected to maximize the single slots ratio to the overall slots, shorter collision slots play a major role in defining $\mathrm{N_{optimal}}$.

In Framed-Slotted ALOHA protocols, several frames are executed until all tags are identified. Depending on the selected frame size N, for a given number of unidentified tags n, the number of collision and empty slots will change. Unidentified tags select their replying slots at random within the given N slots. Accordingly, collision probability in such protocols depends on the number of tags and the frame size.

Since the tags randomly select replying slots, the number of replying tags per slot x, in a given frame $\mathrm{N_k}$, follows a binomial distribution and can be expressed as

$$\mathrm{P(x)} = \binom{\mathrm{n}}{\mathrm{x}} \left(\frac{1}{\mathrm{N_k}}\right)^{\mathrm{x}} \left(1 - \frac{1}{\mathrm{N_k}}\right)^{\mathrm{n-x}}.$$

Therefore, by considering the exponential function approximation formula, $\mathrm{e^x} = \lim_{\mathrm{n}\to\infty}(1 - (\mathrm{x}/\mathrm{n}))^{\mathrm{n}}$, the expected number of $\mathrm{R_e}$, $\mathrm{R_s}$, and $\mathrm{R_c}$ slots will respectively be

$$\mathrm{R_e} = \mathrm{N_k P(0)} = \mathrm{N_k}\left(1 - \frac{1}{\mathrm{N_k}}\right)^{\mathrm{n}} \approx \mathrm{N_k e^{-\psi}}, \tag{12}$$

$$\mathrm{R_s} = \mathrm{N_k P(1)} = \mathrm{N_k}\left(1 - \frac{1}{\mathrm{N_k}}\right)^{\mathrm{n}} - 1 \approx \mathrm{n e^{-\psi}}, \tag{13}$$

and

$$\mathrm{R_c} = \mathrm{N_k} - \mathrm{R_e} - \mathrm{R_s} \approx \mathrm{N_k}\left(1 - (1+\psi)\,\mathrm{e^{-\psi}}\right), \tag{14}$$

where ψ is $\mathrm{n/N_k}$.

If all slots are assumed to have the same length ($\beta = \gamma = 1$), the optimal time efficiency is achieved when the frame size is equal to the tag population [23], $\mathrm{N_{optimal}} = \mathrm{n}$ as depicted in the point P_1 in Fig. 8. By utilizing MS in ALOHA-Based protocols, $\mathrm{N_{optimal}}$ is no longer equal to n. To illustrate this effect, $\mathrm{TSE_g}$ is plotted for ALOHA-based protocols with: i) all slots are of same duration ($\beta = \gamma = 1$), ii) early ending of empty slots ($\beta = 5\%, \gamma = 1$), and iii) MS to end collision and empty slots ($\beta = 5\%, \gamma = 10\%$). Clearly, $\mathrm{TSE_g}$ peaks at different frame sizes and there is a need for a formula that take into account β and γ values in determining $\mathrm{N_{optimal}}$.

By substituting $\mathrm{R_e}$, $\mathrm{R_s}$, and $\mathrm{R_c}$ in the $\mathrm{TSE_g}$ equation, the optimal frame size $\mathrm{N_{optimal}}$ (at which $\mathrm{TSE_g}$ peaks) can be obtained when $d\mathrm{TSE_g}/d\mathrm{N}$ is zero, which is given by

$$\mathrm{nNe^{-\frac{n}{N}}}\left(\gamma(\mathrm{N-n}) + \mathrm{Ne^{-\frac{n}{N}}}(\beta-\gamma)\right) = 0.$$

With

$$\left(\gamma(\mathrm{N-n}) + \mathrm{Ne^{-\frac{n}{N}}}(\beta-\gamma)\right) = 0,$$

we can rearrange the terms as

$$\gamma(\mathrm{n-N}) = \mathrm{Ne^{-\frac{n}{N}}}(\beta-\gamma),$$

which can be further simplified as

$$\frac{(\mathrm{n-N})}{\mathrm{N}}\,\mathrm{e^{\frac{n}{N}}} = \frac{(\beta-\gamma)}{\gamma}.$$

By multiplying both sides of the latter equation by e^{-1} we obtain

$$\frac{(\mathrm{n-N})}{\mathrm{N}}\,\mathrm{e^{(\frac{n-N}{N})}} = \frac{(\beta-\gamma)}{\mathrm{e}\gamma}.$$

The form in the last equation is similar to Lambert W() function [24] such that $\mathrm{W(Y)} = \mathrm{X} \Leftrightarrow \mathrm{Y} = \mathrm{Xe^X}$ with

$$\mathrm{X} = \frac{\mathrm{n-N}}{\mathrm{N}} \quad \text{and} \quad \mathrm{Y} = \frac{(\beta-\gamma)}{\mathrm{e}\gamma}.$$

Hence, the optimal frame size for any value of $\gamma \leq 1$ and $\beta \leq 1$, can be expressed as

$$\mathrm{N_{optimal}} = \frac{\mathrm{n}}{\mathrm{W}\left(\frac{\beta-\gamma}{\mathrm{e}\gamma}\right) + 1}, \tag{15}$$

Equation (15) provides a closed-form expression of the optimal frame size for any framed ALOHA protocol. This closed-form will be used in determining the optimal frame size in our analysis of DFSA protocols.

C. Simulation Setup

In our simulations, we evaluate the state of the art ALOHA- and Tree-based anti-collision protocols under the different possible values of β and γ. Simulation results are also supported by analytical solution to verify the obtained performance results. For the simulation, a tag population in the set $P = [10, 20, 30, \ldots, 4000]$ is considered. For each protocol, every population in P is identified 25 times and the average is reported in the plots of $\mathrm{TSE_g}$ and TH.

In our evaluation, the time slot structure is based on the *data-fields* and *timing* of the EPC standard specifications [13].

The *data-fields* of empty, collision, and single slots are presented in Fig. 9 for NEE, EEE, and MS scenarios. Note that the single slot in MS is slightly longer than single slots of NEE and EEE because of the additional L random sequence. To determine the actual time duration of each slot in Fig. 9, the timing of each field in the slot is required. The key *timing* parameters that determine the slot length are: (1) Tag to reader symbol duration, $\mathrm{T_{pri}}$, which is a function both encoding method and

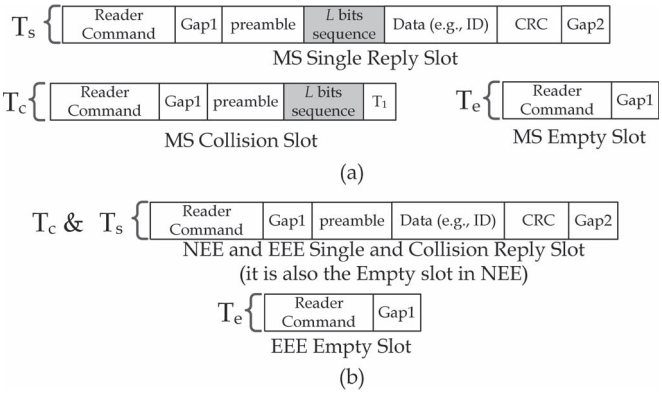

Fig. 9. Single, collision, and empty slots data fields in (a) MS and (b) NEE and EEE.

TABLE II
POSSIBLE COMBINATIONS OF SLOT TIMING PARAMETERS

Settings #	T_{ari} (μs)	Encoding	Divide Ratio
1	6.25	MM2	8
2	6.25	MM2	64/3
3	6.25	FM0	8
4	6.25	FM0	64/3
5	25	MM2	8
6	25	MM2	64/3
7	25	FM0	8
8	25	FM0	64/3

TABLE III
β, γ, AND SINGLE SLOT DURATION FOR THE 8 SETTINGS FROM TABLE II WITH MESSAGE LENGTH OF 144 BITS

	Settings number							
	1	2	3	4	5	6	7	8
Single slot MS (ms)	1.48	0.62	0.83	0.38	5.89	2.44	3.30	1.47
Single-NEE and -EEE(ms)	1.42	0.60	0.80	0.37	5.64	2.35	3.18	1.42
β-NEE(%)	100	100	100	100	100	100	100	100
β-EEE(%)	9.8	19.4	17.3	31.7	9.2	18.1	16.3	29.9
β-MS(%)	9.4	18.6	16.7	30.7	8.8	17.4	15.7	28.9
γ-NEE(%)	100	100	100	100	100	100	100	100
γ-EEE(%)	100	100	100	100	100	100	100	100
γ-MS(%)	11.2	20.3	19.9	33.5	10.7	19.1	19.0	31.8

the Divide Ratio. (2) Reader to tag symbol duration, T_{ari}, (used in the Reader Command field in Fig. 9).

A set of the possible combinations are presented in Table II that considers different combinations of T_{ari} and T_{pri}. Note that T_{pri} is dependent on both encoding methods and divide ratio (DR). The different combinations of the above parameters result in different possible slot lengths, and consequently, different values of β and γ. The resultant β and γ values for the 8 settings from Table II are presented in Table III.

D. MS in ALOHA-Based Protocols

1) MS Effect on DFSA-Based Protocols: In Fig. 10 TSE_g and TH for DFSA protocol are evaluated by simulating tag identification under the three scenarios of EEE, NEE, and MS. As the frame length is limited to a maximum value N_{max} [22],

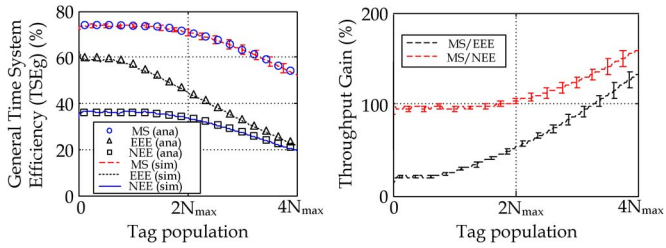

Fig. 10. TSE_g and Throughout gain for DFSA protocol with MS (γ and β less than 1), Empty slot Early ending (β less than 1), and non-MS ($\gamma = \beta = 1$) according to the timing parameters combinations in Table II.

$N_{optimal} = \min(N_{optimal}, N_{max})$. Tag population is changed from 5 tags to $4N_{max}$ tags. To verify the simulations, we have plotted the analytical gain of MS from (8)–(11). The simulated and analytical results are denoted as (sim) and (ana), respectively.

Note that the simulated and analytical results match perfectly. The performance of DFSA in Fig. 10 considers the average of the different possible tag-to-reader bit length (T_{pri}) and the reader-to-tag bit length (T_{ari}) combinations. The simulated results of MS have error bars. The upper limit represent MS when collisions are early-detected at preamble of the time slot (in the case of Unsynchronized Transmissions, denoted as UT in this plot and the following plots), while the lower limit represents collision detection within the L random sequence for bit level Synchronized Transmissions (denoted as ST).

At low tag population, the performance of DFSA with MS shows a stable improvement of 15% and 38% over EEE and NEE, respectively. This is because the contribution of collision slots is minimal when the frame size is larger than the tag population. At higher tag population, the collision starts to be more dominant, as N_{max} is smaller than tag population, showing a significant improvement of MS over EEE and NEE. In addition, MS performance indicates immunity to performance degradation when collision slots dominate the frame slots. Note that the throughput gain of MS over NEE is much higher than MS over EEE (at small tag populations). This is because EEE (similar to MS) eliminates the effect of empty slots at frames with low tag population. For higher populations, the throughput gain converges as collision slots are dominating and the effect of ending empty slots is negligible.

2) MS Effect on Q-Algorithm Protocols: In Q-Algorithm ALOHA-based protocols [3], [13], the frame sizes are $2^{\lfloor Q \rfloor}$ slots, where Q is a number that varies by the constant c (where $0.1 \leq c \leq 0.5$). The value of Q increases after each collision slot (i.e., $Q_{new} = Q + c$), and it decreases by c after an empty slot. Once the new value of $\lfloor Q_{new} \rfloor \neq \lfloor Q \rfloor$, a new frame with $2^{Q_{new}}$ slots is issued. Note that the optimal frame is not considered in the Q-Algorithm. The Q-algorithm rather regulates the frame size to equalize the probability of collision and empty slots as shown in Q-algorithm simulation in Fig. 11. In Fig. 11, the total numbers of collision and empty slots are equal to single slots (i.e., $a = 1$ and $b = 1$ in (5)–(11)).

In our simulations, MS significantly enhances TSE_g over both NEE and EEE in the eight timing settings as depicted in Fig. 12(a). As in the plot of DFSA, TSE_g columns of MS in Fig. 12(a) represent UT and ST bounds. MS average

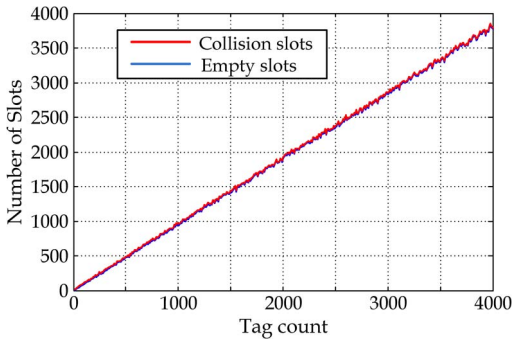

Fig. 11. The total collision slots and empty slots in Q-algorithm [13], [25].

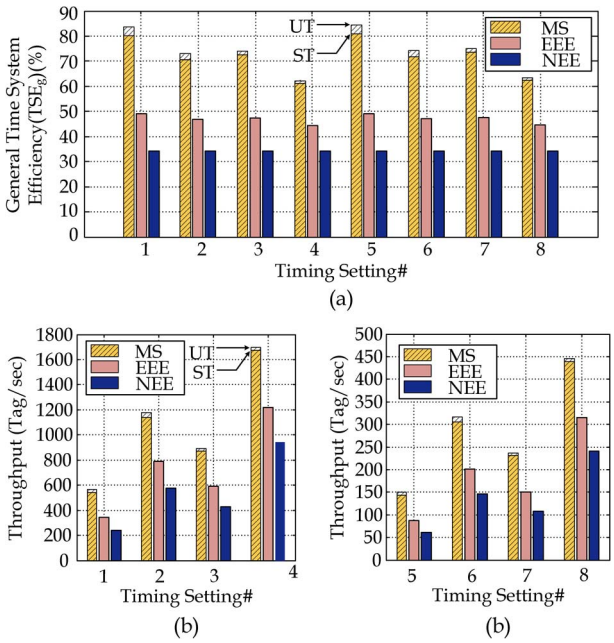

Fig. 12. Performance of ALOHA-based Q-algorithm systems with NEE, EEE, SM. (a) TSE_g. (b), (c) Throughput.

improvement of TSE_g over NEE and EEE is 110% and 56%, respectively. These percentages agree with Eqs. (8) and (10) with $a = 1$, $b = 1$, and $L = 8$ bits for w and z.

The throughput of Q-algorithm for all timing settings is plotted in Fig. 12(b) and (c). Significant improvements in the throughput is achieved by applying MS to the Q-algorithm. On average, the throughput enhancement is 120% and 53% over NEE and EEE, respectively, which also agrees to the analytical solution in Eqs. (9) and (11).

E. MS Effect on Tree-Based Protocols

1) MS in Binary Tree: Collision contribution in Tree-based protocols is proportional to the tag population (collision slots have a fixed ratio to the total slots) [4], [5], [25]. Table IV presents collision and empty slots contribution in binary Tree-based protocols [5]. In our simulations, we consider the longer reader message since the command in Tree-based protocols has extra bits that are appended after the reader's command for prefix matching purposes. When MS is compared for a scenario with an unknown tag population, an enhancement of 140% and 130% is achieved in TSE_g and TH, respectively. For the same scenario, when MS is compared to EEE, TSE_g, and TH are doubled. For a known tag population, MS doubles the TSE_g and the throughput of NEE systems and increases the throughput of EEE by more than 46.4%. Similar improvement is obtained for the rest of the time settings of Table III.

TABLE IV
R_s, R_e, AND R_c CONTRIBUTION IN BINARY TREE-BASED PROTOCOLS [5]

Scenario	Collision slots	Empty slots	Single slots
Unknown n	$1.443R_s$	$0.442R_s$	R_s
Known n	$0.669R_s$	$0.669R_s$	R_s

TABLE V
SUMMARY OF TSE_g AND TH IN Q-ALGORITHM AND BINARY TREE-BASED PROTOCOLS

Protocol	MS		EEE		NEE	
	TSE_g	TH	TSE_g	TH	TSE_g	TH
Q-Algorithm	72%	665	46%	449	33%	334
Tree (Unknown)	74%	671	39%	392	34%	346
Tree (Known)	81%	739	55%	547	43%	427

In Table V, a summary of average TSE_g and TH (in tags per second) values form ALOHA-based Q-Algorithm protocol and Binary Tree-based protocol (known and unknown tag populations) simulations for MS, NEE, and EEE. The reported results also agree with Eqs. (5)–(7).

F. Discussion

In the following we discuss the potential power saving by MS and its effect on robust throughput in the presence of estimation errors.

1) Power Consumption: Although the focus in this paper lies on temporal analysis of MS, we also expect a potential reduction in power consumption at the reader. As the reader's RF interface is powered ON during both command transmission and tag reply reception [6], a reduction in the overall reading time is expected to cause a similar reduction in the battery depletion rate.

2) Robustness to Estimation Errors: In ALOHA-based protocols, tag population is estimated based on the statistics of empty, single, and collision slots statistics from previous frames [11], [23]. Therefore, with unavailable statistics for estimating the first frame, high estimation errors are inevitable. MS does not only enhance the time efficiency of ALOHA-based protocols, but also increases the robustness of systems prone to errors in frame size estimation. Fig. 13 shows the time efficiency behavior of MS, EEE, NEE systems for tag population that is much smaller than the frame size to tag population that are 3.9 times the frame size. TSE_g curve for MS is significantly robust over NEE and EEE to non-optimal frame sizes. For instance, if the error tag estimation spans twice the actual population, TSE_g of MS is at least 70% (which is higher than the peak of EEE). For the same estimation error, EEE and NEE performance will drop below 30% and 22%, respectively. With MS, rough and less complex estimation function can be executed while maintaining the same performance figure.

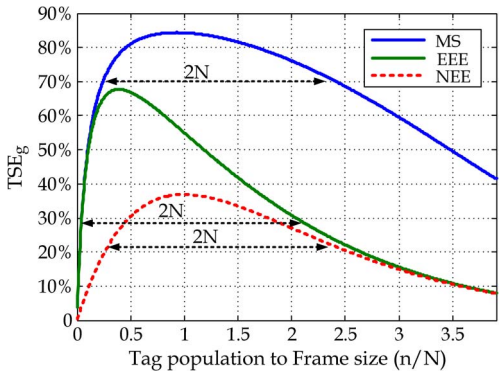

Fig. 13. The performance of MS ($\beta = 0.1, \gamma = 0.12$), EEE ($\beta = 0.1$, $\gamma = 1$), and NEE ($\beta = \gamma = 1$) for tag population from 0 to 3.9 times the frame size.

V. Conclusion

Collision between tags replies is a major limiting factor of time efficiency in tag identification protocols. In this paper, we addressed the time reduction of collision slots in RFID systems. We proposed a new tag-reader interaction mechanism, Modulation Silencing (MS), which allows the reader to silence the tags if a collision is detected. Modulation silencing is achieved by the reader-tag coordination to reduce the total reading time with minimal modification to the tag's IC chip. The analytical solutions and extensive simulations verified the significance of MS in RFID systems. MS is capable of raising the efficiency of ALOHA-based RFID systems to 80% while non-MS are limited to 36.4%. In Tree-based protocols, shorter collision slots by MS doubles the time efficiency for unknown and known tag count.

MS is not limited to anti-collision protocols; the ability of silencing the tag at any point during transmission is novel and can be applied in numerous applications. MS can be utilized in improving tag counting systems. In such systems, the type of slot (single, empty, or collision) is more important than the tag's message. Once the type of slot is defined, the reader ends it by MS. A second front of applications can be tag authentication protocols. To limit the available information from eavesdroppers, the reader can utilize a tree-based hashing mechanism; the reader keeps receiving the hashed stream from the tag until it can determine the next branch. Once the reader has determined the next branch it can silence the tag and wait for the next hashed value.

References

[1] K. Finkenzeller, *RFID Handbook: Fundamentals and Applications in Contactless Smart Cards and Radio Frequency Identification and Near-Field Communication*, 3rd ed. Hoboken, NJ, USA: Wiley, 2010.

[2] T. La Porta, G. Maselli, and C. Petrioli, "Anticollision protocols for single-reader RFID systems: Temporal analysis and optimization," *IEEE Trans. Mobile Comput.*, vol. 10, no. 2, pp. 267–279, Feb. 2011.

[3] D. Klair, K.-W. Chin, and R. Raad, "A survey and tutorial of RFID anti-collision protocols," *IEEE Commun. Surveys Tuts.*, vol. 12, no. 3, pp. 400–421, 2010.

[4] L. Pan and H. Wu, "Smart trend-traversal protocol for RFID tag arbitration," *IEEE Trans. Wireless Commun.*, vol. 10, no. 11, pp. 3565–3569, Nov. 2011.

[5] D. Hush and C. Wood, "Analysis of tree algorithms for RFID arbitration," in *Proc. IEEE Int. Symp. Inf. Theory*, Aug. 1998, p. 107.

[6] D. Dobkin, *The RF in RFID: Passive UHF RFID in Practice*. Newton, MA, USA: Newnes, 2007.

[7] C. Boyer and S. Roy, "Backscatter communication and RFID: Coding, energy, MIMO analysis," *IEEE Trans. Commun.*, vol. 62, no. 3, pp. 770–785, Mar. 2014.

[8] P. Cole, "Fundamentals in radio frequency identification," Auto-ID Res. Lab., Adelaide, SA, Australia, Tech. Rep., Mar. 2004.

[9] L. Xie *et al.*, "Efficient tag identification in mobile RFID systems," in *Proc. IEEE INFOCOM*, Mar. 2010, pp. 1–9.

[10] Y. Zheng and M. Li, "PET: Probabilistic estimating tree for large-scale RFID estimation," *IEEE Trans. Mobile Comput.*, vol. 11, no. 11, pp. 1763–1774, Nov. 2012.

[11] B. Knerr, M. Holzer, C. Angerer, and M. Rupp, "Slot-wise maximum likelihood estimation of the tag population size in FSA protocols," *IEEE Trans. Commun.*, vol. 58, no. 2, pp. 578–585, Feb. 2010.

[12] MIT Auto-ID Center, "13.56 MHz ISM band class 1 radio frequency identification tag interface specification: Candidate recommendation, version 1.0.0," Adelaide, SA, Australia, Tech. Rep., Feb. 2003.

[13] *EPC Radio-Frequency Identification Protocols Class-1 Gen-2 UHF RFID Protocol for Communications at 860 MHz–960 MHz*, EPCglobal Std. Rev. 1.2.0, Oct. 2008.

[14] L. Kang, K. Wu, J. Zhang, H. Tan, and L. Ni, "DDC: A novel scheme to directly decode the collisions in UHF RFID systems," *IEEE Trans. Parallel Distrib. Syst.*, vol. 23, no. 2, pp. 263–270, Feb. 2012.

[15] R. Khasgiwale, R. Adyanthaya, and D. Engels, "Extracting information from tag collisions," in *Proc. IEEE Int. Conf. RFID*, Apr. 2009, pp. 131–138.

[16] J. Li and Y. Huo, "An efficient time-bound collision prevention scheme for RFID re-entering tags," *IEEE Trans. Mobile Comput.*, vol. 12, no. 6, pp. 1054–1064, Jun. 2013.

[17] Y. Cui and Y. Zhao, "Performance evaluation of a multi-branch tree algorithm in RFID," *IEEE Trans. Commun.*, vol. 58, no. 5, pp. 1356–1364, May 2010.

[18] A. Alma'aitah, H. Hassanein, and M. Ibnkahla, "Modulation silencing: Novel RFID anti-collision resolution for passive tags," in *Proc. IEEE Int. Conf. RFID*, Apr. 2012, pp. 81–88.

[19] J.-P. Curty, N. Joehl, C. Dehollaini, and M. Declercq, "Remotely powered addressable UHF RFID integrated system," *IEEE J. Solid-State Circuits*, vol. 40, no. 11, pp. 2193–2202, Nov. 2005.

[20] R. Chakraborty, S. Roy, and V. Jandhyala, "Revisiting RFID link budgets for technology scaling: Range maximization of RFID tags," *IEEE Trans. Microw. Theory Tech.*, vol. 59, no. 2, pp. 496–503, Feb. 2011.

[21] J. Griffin and G. Durgin, "Complete link budgets for backscatter-radio and RFID systems," *IEEE Antennas Propag. Mag.*, vol. 51, no. 2, pp. 11–25, Apr. 2009.

[22] J. Park, M. Chung, and T. Lee, "Identification of RFID tags in framed-slotted ALOHA with robust estimation and binary selection," *IEEE Commun. Lett.*, vol. 11, no. 5, pp. 452–454, May 2007.

[23] H. Vogt, "Multiple object identification with passive RFID tags," in *Proc. IEEE Int. Conf. Systems, Man Cybern.*, Oct. 2002, vol. 3, pp. 1–6.

[24] R. Corless, G. Gonnet, D. Hare, D. Jeffrey, and D. Knuth, "On the Lambert W function," *Adv. Comput. Math.*, vol. 5, no. 1, pp. 329–359, 1996.

[25] H. Wu, Y. Zeng, J. Feng, and Y. Gu, "Binary tree slotted ALOHA for passive RFID tag anticollision," *IEEE Trans. Parallel Distrib. Syst.*, vol. 24, no. 1, pp. 19–31, Jan. 2012.

Abdallah Alma'aitah (M'13) received the B.Sc. degree in computer engineering from Mu'tah University, Jordan, in 2005 and, the M.Sc. degree in electrical and computer engineering from the University of Western Ontario, Canada, in 2008, and the Ph.D. degree in electrical and computer engineering from Queen's University, Canada, in 2013. He is currently a term Adjunct Assistant Professor at the Electrical and Computer Engineering Department and a post-doctoral fellow at the School of Computing at Queen's University.

His current research interests are in the broad area of wireless communications and smart environments. In particular, his focus is on embedded systems power optimization, large scale deployment of RFID systems and wireless sensors networks in harsh environments, and wireless power transfer for Internet of Things (IoT).

Dr. Alma'aitah is the recipient of R.S. McLaghlin Award for the years 2011, 2012, and 2013, and Queen's University graduate award from 2008 until 2012.

Hossam S. Hassanein (SM'05) is leading research in the areas of wireless and mobile networks architecture, protocols and services. His record spans more than 500 publications in journals, conferences and book chapters, in addition to numerous keynotes and plenary talks in flagship venues. Dr. Hassanein has received several recognition and best papers awards at top international conferences. He is also the founder and director of the Telecommunications Research Lab at Queen's University School of Computing, with extensive international academic and industrial collaborations. He is a former chair of the IEEE Communication Society Technical Committee on Ad hoc and Sensor Networks (TC AHSN). Dr. Hassanein is an IEEE Communications Society Distinguished Speaker (Distinguished Lecturer 2008–2010).

Mohamed Ibnkahla (M'95) received the engineering degree in electronics and the Diplome d'Etudes Approfondies degree (equivalent to M.Sc.) in signal and image processing in 1992, the Ph.D. degree in 1996, and the Habilitation a Diriger des Recherches degree (HDR) in 1998, all from the National Polytechnic Institute of Toulouse (INP), Toulouse, France. He currently holds a Full Professor position at the Department of Electrical and Computer Engineering, Queen's University, Kingston, ON, Canada. He was previously an Assistant Professor at INP (1996–1999) and Queen's University (2000–2004) and Associate Professor at Queen's University (2004–2012). He is also the founding Director of the Wireless Communications and Signal Processing Laboratory (WISIP) at Queen's University. He has published the following books: Signal Processing for Mobile Communications Handbook (London, U.K.: Taylor & Francis/CRC Press, 2004), Adaptive Signal Processing in Wireless Communications (London, U.K.: Taylor & Francis/CRC Press, 2008), Adaptive Networking and Crosslayer Design in Wireless Networks (London, U.K.: Taylor & Francis/CRC Press, 2008), Wireless Sensor Networks: A Cognitive Perspective (London, U.K.: Taylor & Francis/CRC Press, 2012), and Cooperative Cognitive Radio Networks: The Complete Spectrum Cycle (London, U.K.: Taylor & Francis/CRC Press, 2014). He has published more than 50 peer-reviewed journal papers and book chapters, 20 technical reports, 100 conference papers, and 4 invention disclosures. His research interests include cognitive radio, adaptive signal processing, cognitive networking, neural networks, and wireless sensor networks and their applications. Dr. Ibnkahla received the INP Leopold Escande Medal in 1997, France, for his research contributions to signal processing; and the prestigious Prime Minister's Research Excellence Award (PREA), Ontario, Canada, in 2001, for his contributions in wireless mobile communications. He is a Registered Professional Engineer (PEng) of the Province of Ontario, Canada.